LOCAL-SCALE STRATIGRAPHY OF GROOVED TERRAIN ON GANYMEDE

Scott L. Murchie, James W. Head, and Paul Helfenstein, Department of Geological Sciences, Brown University, Providence, RI 02912, and Jeffrey B. Plescia, U.S. Geological Survey, Flagstaff, AZ 86001.

The surface of Ganymede is divided into two major units, dark terrain cut by arcuate and subradial furrows, and light terrain consisting largely of areas with pervasive U-shaped grooves (grooved terrain) (1,2). The grooved terrain may be subdivided on the basis of pervasive morphology of groove domains into four terrain types (3): (*a*) elongate bands of parallel grooves (*groove lanes*); (*b*) polygonal domains of parallel grooves (*grooved polygons*); (*c*) polygonal domains of two orthogonal groove sets (*reticulate terrain*); and (*d*) polygons having two to several complexly cross-cutting groove sets (*complex grooved terrain*). Reticulate terrain is frequently dark and not extensively resurfaced, and grades to a more hummocky terrain type. The other three grooved terrain types have almost universally been resurfaced by light material during their emplacement (1,2,3,4,5).

The sequence of events during grooved terrain emplacement has been investigated by Lucchitta (4), who suggested that reticulate terrain is an intermediate stage in the conversion of dark terrain into light grooved terrain. Golombek and Allison (6) proposed that groove lanes dissect older dark terrain into polygonal blocks that are later resurfaced and fractured to form grooved polygons. In this study, we attempt to integrate observed geologic and tectonic patterns to better constrain the relative ages and styles of emplacement of grooved terrain types. A revised model of grooved terrain emplacement is proposed and is tested using detailed geologic mapping and measurement of crater-density.

Important spatial and temporal tectonic patterns in grooved terrain include (*a*) structural control of grooves, whose orientations are closely related to the regional orientations of older, arcuate and radial furrows (3), (*b*) the correspondence of global groove lane orientations with the pattern predicted for reactivated tidal despinning fractures (7), (*c*) similar sizes and shapes of nearby polygons of different terrain types, and (*d*) evidence for emplacement of light terrain as shallowly resurfaced downdropped blocks (4,8). Narrow dark troughs are observed to widen into groove lanes, and exhibit a longitudinal sequence of (*a*) initial trough formation, (*b*) patchy discontinuous resurfacing, and (*c*) extensive resurfacing and pervasive groove formation, interpreted here to imply a sequence of initial extension followed by ice volcanism. The groove lanes are similar in plan to continental rifts, and Murchie *et al.* (9) proposed that they are passive rifts driven by global expansion. Concentration of grooved polygons and reticulate terrain between closely spaced groove lanes suggests that polygonal blocks were deformed where the lithosphere had been thinned, as it may be on earth (10), between closely spaced rifts. This hypothesis is consistent with the inference of Grimm and Squyres (11) that lithospheric thinning occurred during the emplacement of grooved terrain. One further very significant tectonic pattern is that groove lanes defining the margins of reticulate and grooved polygons also bury and cross-cut grooves within the polygons. This relationship implies that many groove lanes developed by reactivation of older structures (grooves or normal faults), that had earlier confined fracturing and the lateral extent of light material emplacement within the deformed polygons.

On the basis of the patterns listed above, we propose the following generalized sequence of events during grooved terrain formation: *stage 1*, dissection of the lithosphere by incipient rifts following preexisting, throughgoing zones of weakness (furrows, relict despinning fractures), accompanied by thinning and probably deformation of intervening blocks as stress is concentrated there; *stage 2*, extensive resurfacing and continued deformation of the polygons; and *stage 3*, repeated reactivation of the throughgoing zones of weakness, which are

deformed preferentially as the lithosphere thickens.

Three areas were investigated in detail to test this model. Results in each case were similar, so only the results from the area of central Uruk Sulcus (5°S-12°N, 145°-160°W, Voyager 2 image 20637.20) will be discussed in detail. A series of detailed maps was prepared, as described in (9), from which relative age units were determined using cross-cutting relations of grooves and superposition relations of light material. The six relative age units are: (*A*) patchily resurfaced reticulate to hummocky terrain, outlined by throughgoing grooves; (*B*) completely but shallowly resurfaced reticulate terrain having highly degraded troughs; (*C*) grooved polygons superposed on *B*; and (*D*, *E*, and *F*) groove lanes and a few grooved/resurfaced polygons. Repeatedly reactivated zones of weakness were identified, that confined both fracturing and light material emplacement within deformed polygons, and also were preferred sites of groove lane formation. In all three terrain types represented in Uruk Sulcus, dominant groove orientations are parallel to older arcuate or radial furrows. Both the groove lanes and the throughgoing zones of weakness have restricted orientations (*a*) nearly parallel to arcuate furrows and (*b*) parallel to inferred relict tidal despinning fractures (7). Smaller groove spacing in the grooved polygons than in groove lanes suggests that the grooved polygons formed when the lithosphere was relatively thinner, as is suggested in the model.

The validity of the sequence of events derived through geologic mapping was tested by measurement of the densities of craters superposed on the six relative age units and on adjacent, older dark furrowed terrain (Table 1). Densities of craters >2 km and >5 km in diameter show that the six relative age units form three larger relative age groupings: *A*, oldest; *B-C*, intermediate age; and *D-F*, youngest. In addition, *E* probably is younger than *D*. Therefore, crater-density measurements corroborate the relative age units derived through geologic mapping. Calibration of the densities using the crater-production curve of (11) shows that the duration of grooved terrain emplacement in Uruk Sulcus was $\geq 10^8$ yrs.

Each of the three major relative age groups (*A*, *B-C*, *D-F*) is dominated by a different terrain type, and the sequence of terrain types is consistent with the generalized 3-stage sequence in the model. *Stage 1* is characterized by formation of throughgoing grooves following preexisting zones of weakness, and by development of reticulate to hummocky terrain in the intervening polygons. *Stage 2* is characterized by resurfacing of the intervening polygons and formation of grooved polygons. During *stage 3*, deformation is concentrated at the sites of initial throughgoing grooves, in the form of repeated groove lane formation.

In summary, we propose that grooved terrain formation at a local scale occurs in $\geq 10^8$ yrs, as a general 3-stage process shown in Figure 1. Preexisting structures exert strong control on orientation and lateral extent of groove sets. A sequence of thinning and later thickening of the lithosphere during grooved terrain emplacement may occur.

REFERENCES: (1) Smith, B., and the Voyager Imaging Team, *Science, 204*, 951-972, 1979*a*. 599-600, 1985. (2) Smith, B., and the Voyager Imaging Team, *Science, 206*, 927-950, 1979*b*. (3) Murchie, S., and J. Head, *Lunar Planet. Sci. XVI*, (4) Lucchitta, B., *Icarus, 44*, 481-501, 1980. (5) Casacchia, R., and R. Strom, *J. Geophys. Res., 89*, B419-B428, 1984. (6) Golombek, M., and M. Allison, *Geophys. Res. Lett., 8*, 1139-1142, 1981. (7) Murchie, S., and J. Head, *Geophys. Res. Lett, 13*, 345-348, 1986. (8) Schenk, P., and W. McKinnon, *J. Geophys. Res., 90*, C775-C783, 1985. (9) Murchie, S., J. Head, P. Helfenstein, and J. Plescia, *J. Geophys. Res.*, in press, 1986. (10) Girdler, R., *Tectonophysics, 94*, 241-252, 1983. (11) Grimm, R., and S. Squyres, *J. Geophys. Res., 90*, 2013-2021, 1985. (12) Shoemaker, E., and R. Wolfe, in *The Satellites of Jupiter*, edited by D. Morrison, pp. 277-239, Univ. of Arizona, Tucson, 1982.

TABLE 1. Cumulative Crater Densities in Uruk Sulcus, $\times 10^{-6}$ km^{-2}

Unit	Area, km^2	>2 km	>5 km	>10 km	>20 km
Furrowed	193,072	–	539 ± 53	238 ± 35	41 ± 15
A	111,689	–	458 ± 64	233 ± 46	47 ± 20
B-C	151,149	992 ± 81	205 ± 37	98 ± 25	37 ± 15
D	87,821	797 ± 95	190 ± 46	98 ± 33	47 ± 23
E	48,435	681 ± 119	123 ± 40	75 ± 40	38 ± 27
F	20,750	723 ± 187	271 ± 112	133 ± 80	–

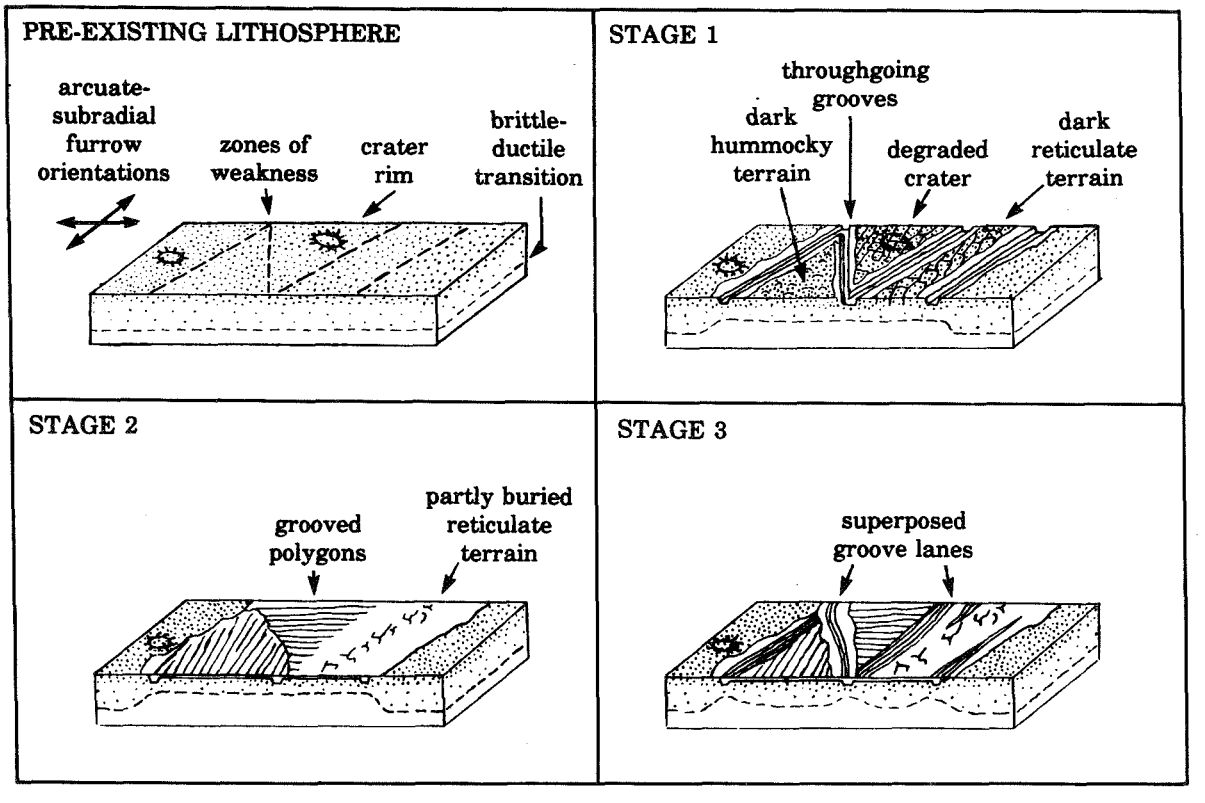

Figure 1. Schematic illustration of the generalized 3-stage sequence of events during grooved terrain formation.